Progress In Electromagnetics Research Letters, Vol. 83, 99–105, 2019

New Ultra-Wideband Filter with Sharp Notched Band Using Defected Ground Structure

Jingbo Liu[1], Wenhao Ding[2], Jianzhong Chen[3, *], and Anxue Zhang[4]

Abstract—An ultra-wideband microstrip bandpass filter which operates from 3.1 GHz to 10.6 GHz, with high selectivity and sharp notched band is presented and experimentally verified. The filter is composed of a square loop shaped defected ground structure, metal faces, and microstrip lines. By adding two short stubs connected by a short circuit point on the microstrip lines, the filter achieves an attractive capacity in out-of-band rejection. By placing open stubs in microstrips, the filter realizes a notched band in passband. To illustrate the possibilities of the new approach, an ultra-wideband microstrip bandpass filter is designed and fabricated. Measured results agree well with the predicted counterparts.

1. INTRODUCTION

Ultra-wideband (UWB) technology has been receiving tremendously increasing attention in high performance communication systems because it successfully overcomes the drawbacks of many classical communication technologies with its high speed, high immunity of noise, and low transmitting power [1]. Corresponding to this trend, various UWB filters with compact size, light weight, and adequate electrical characteristic performances have been extensively studied and explored [2]. One of the design techniques for obtaining high performance microwave filters is using defected ground structure (DGS) [3] resonators which are typically etched as various shaped breaks in the ground plane. DGSs act as parallel L-C resonators which resonate at certain frequencies depending on their dimensions and shapes for harmonic suppression [4–6].

UWB filters using DGS are always smaller than general UWB filters using multi-mode resonators in size and easy to manufacture. Moreover, rejection band is typically wider, and multi-pole characteristic can be set with combining several multimode resonators that have different sizes or shapes for harmonic suppression [7–10]. In this paper, a new UWB bandpass filter is proposed and implemented based on DGS. The proposed square ring shaped DGS is positioned symmetrically between the ports on the ground plane of initial filter. Hence, the filter itself is composed of dual metal faces and dual microstrip lines with short stubs to enhance out-of-band rejection and open stubs to create a notched band in passband. In the design process, the performance of BPF with the proposed DGS is investigated intensively to obtain the optimum design of overall structure. A UWB BPF with compact size and high performance is then presented, and predicted results are experimentally verified by testing the fabricated filter.

Received 13 November 2018, Accepted 18 December 2018, Scheduled 10 April 2019

* Corresponding author: Jianzhong Chen (jianzhong.chen@xjtu.edu.cn).

[1] China Railway Qinghai-Tibet Group Co., Ltd, Xining, Qinghai 810007, P. R. China. [2] Henan Thinker Rail Transit Technology Research Institute Company, Ltd, Zhengzhou, Henan 450001, P. R. China. [3] School of Electronic and Engineering, Xidian University, Xi'an, Shaanxi 710071, P. R. China. [4] School of Electronic and Information Engineering, Xi'an Jiaotong University, Xi'an, Shaanxi 710049, P. R. China.

2. PRINCIPLE AND FILTER DESIGN

Figure 1(a) depicts a UWB filter on a uniform impedance DGS square ring as its ground, with a pair of metal faces linking to port 1 and port 2 via microstrip lines. The microstrip-line-transmission characteristic impedances of the metal faces are Z_1 and Z_2, with their corresponding electric lengths of microstrips being θ_1 and θ_2, and widths of W_1 and W_2. The DGS square ring has the electric length of θ_3 for the horizontal arms and θ_4 for the vertical arms, with characteristic impedance of Z_3 and width of W_3. The simulated responses with $L_1 = 8.5\,\text{mm}$, $L_2 = 4.9\,\text{mm}$, $L_3 = 10.4\,\text{mm}$, $L_4 = 5.4\,\text{mm}$, $g = 0.2\,\text{mm}$, $W_1 = 2.3\,\text{mm}$, $W_2 = 1\,\text{mm}$, and $W_3 = 0.4\,\text{mm}$ are plotted in Fig. 1(b). As illustrated in Fig. 1(b), a transmission zero at the right side of the passband sharpens the out-of-band rejection skirt, and a high performance UBW BPF is achieved. Figs. 2(a), (h) illustrate frequency responses with each variable quantity while the others are constant. The simulation in this paper is carried out in the EM software Zeland IE3D.

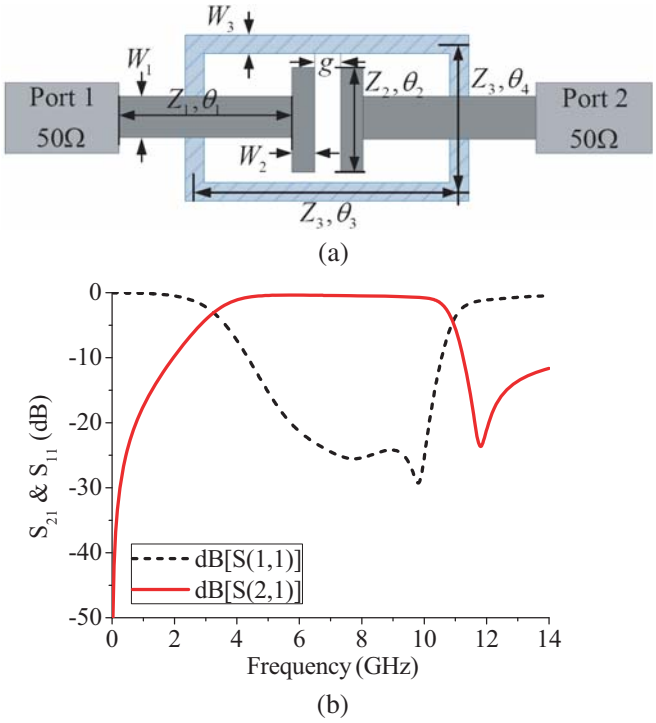

Figure 1. (a) Layout of the ultra wideband filter with DGS loop structure. (b) Simulated responses of the ultra wideband filter.

As can be seen, the transmission zero at right side of the passband performs a right shift with the increase of L_3, W_3, g, and W_2. At the same time, the out-of-passband rejection at transmission zero is enhanced with the decrease of L_2 and W_1, as well as increase of L_4.

To enhance the left side out-of band rejection without affecting these specified in-band frequency responses, a transmission zero would be introduced at the left side of passband. As shown in Fig. 3(a), dual short-circuit lines connected by a short-circuit point were added on the microstrip-lines. Fig. 3(b) shows the simulated frequency responses of the new filter with the same size in Fig. 1(a) where $d_1 = 4.05\,\text{mm}$, $d_2 = 4.05\,\text{mm}$, $W_4 = 0.4\,\text{mm}$, $D = 0.8\,\text{mm}$, $a = 1.2\,\text{mm}$, and $L_S = 7.5\,\text{mm}$. As illustrated in Fig. 3(b), a new transmission zero at 1.42 GHz enhances the left side out-of-band rejection.

As shown in Fig. 4, the simulated frequency responses vary under three different shot-circuit lines' lengths. As can be remarkably identified, the right side out-of-band rejection is enhanced with increment of shot-circuit lines' lengths from 7.5 mm to 9.5 mm while the left side rejection level will be degraded when the shot-circuit lines' lengths become longer. Furthermore, the right side out-of-band rejection is greater than 10 dB over a frequency range of 11–16 GHz when shot-circuit lines' lengths are 8.5 mm or longer. In such cases, the shot-circuit-lines affect both right and left side out-of-band rejections.

As we know, introducing an in-band transmission zero by adding open-circuit lines would create a notched band in passband. The open-lines with one side linking to the ports were added via grooves on microstrip lines in Fig. 5(a). The width and length of the grooves are W_5 and L_5, and their distances to the open-circuit lines are S. In such cases, the open-circuit lines can be considered as $\lambda_g/4$ transmission lines. Furthermore, the open-circuit lines' length L_O and width W_O would decide the central frequency and the relative bandwidth of the stop-bands. However, the grooves would influence in-band frequency responses. As can be remarkably identified in Fig. 5(b), the amplitudes of in-band standing wave flattened and the out-of-band rejection were enhanced with grooves of size: $W_5 = 1\,\text{mm}$, $L_5 = 6.3\,\text{mm}$; at the same time $|S_{21}\,(\text{dB})| > 10\,\text{dB}$ at the right side out-of-band over a frequency range of 11–14 GHz. The grooves create a new transmission zero marked as TZ, which improves the out-of-band rejection and frequency responses performance.

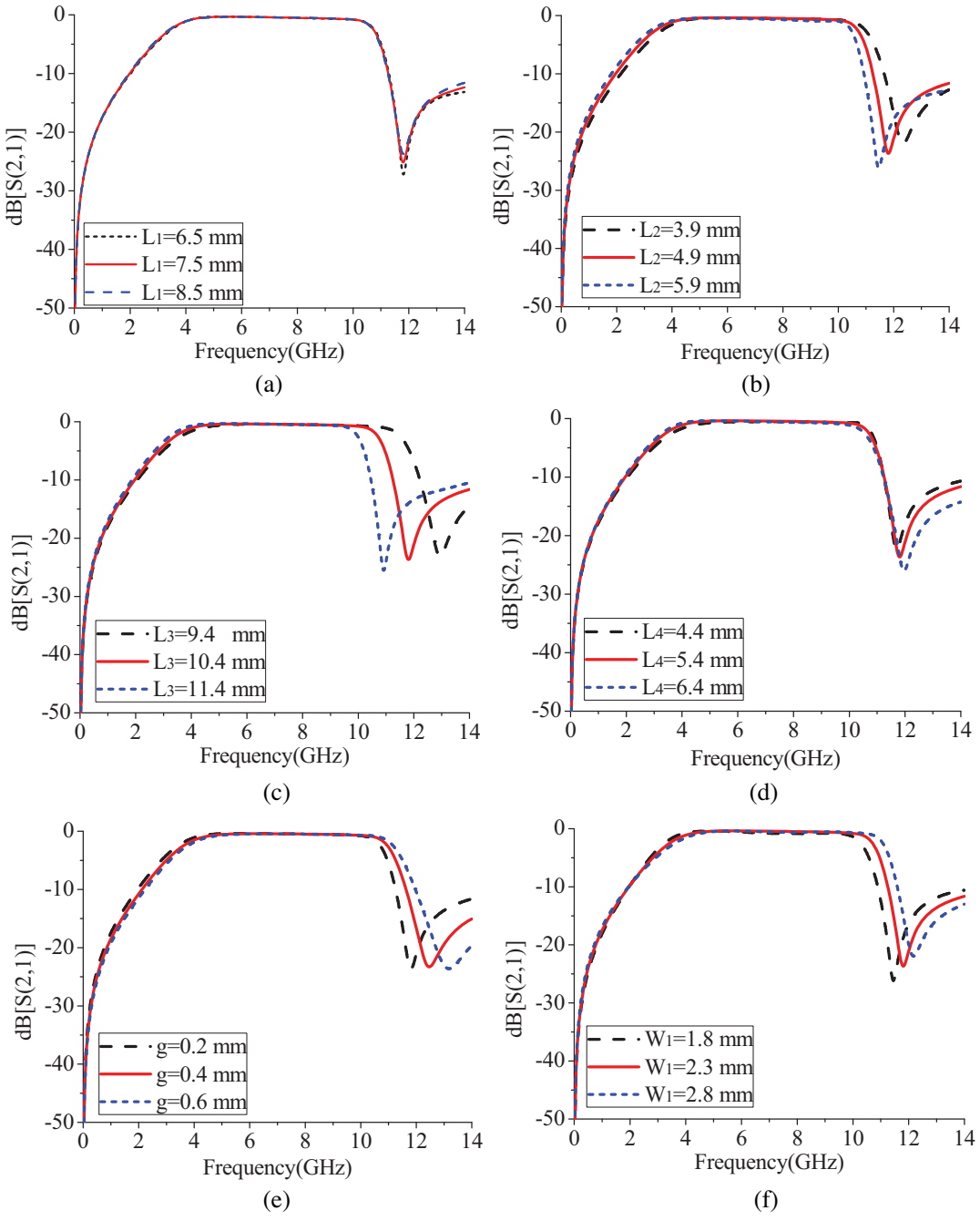

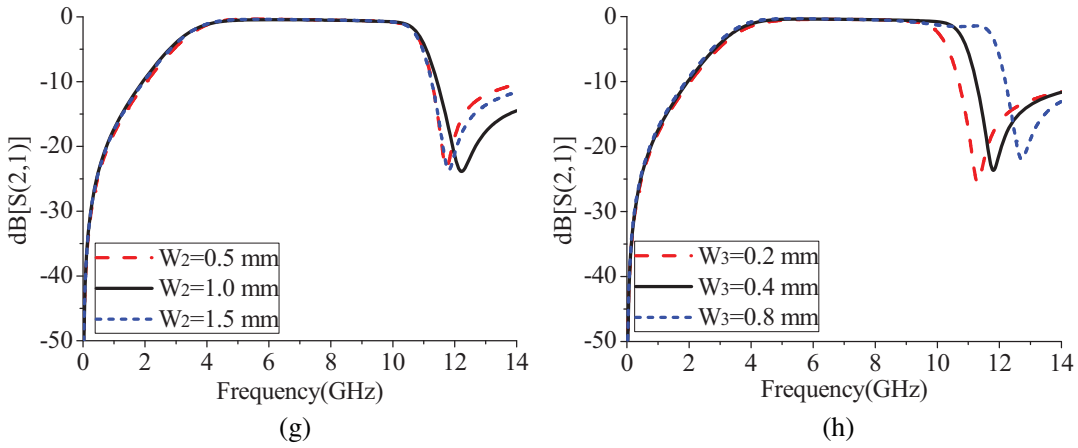

Figure 2. (a)–(h) Frequency responses with each one variable quantity while the others are constant: (a) L_1, (b) L_2, (c) L_3, (d) L_4, (e) g, (f) W_1, (g) W_2, (h) W_3.

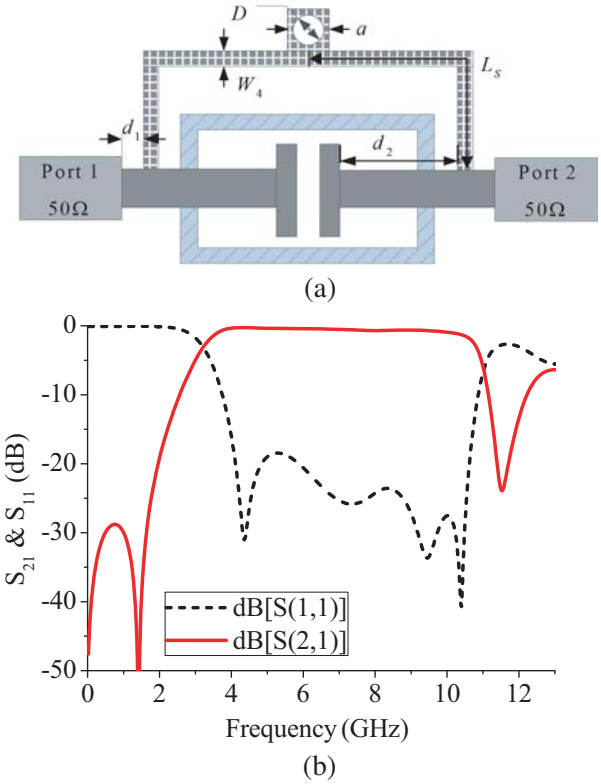

Figure 3. (a) Layout of ultra wideband filter with short-circuit lines. (b) Simulated frequency responses of S-parameters.

The simulated frequency responses with varied L_5 and W_5 are shown in Fig. 6. As can be identified in Fig. 6(a), the frequency of TZ becomes lower, and its attenuation gets higher with increment of grooves length from 5.3 mm to 7.3 mm. The in-band transmission will become worse when TZ gets close to the passband. So the length of grooves L_5 should be appropriately chosen. As can be identified in Fig. 6(b), the in-band standing wave is raised with increment of grooves width from 0.5 mm to 1.8 mm. The reason is that the transmission lines become high-impedance lines, and the ports become impedance mismatch with the increment of grooves width.

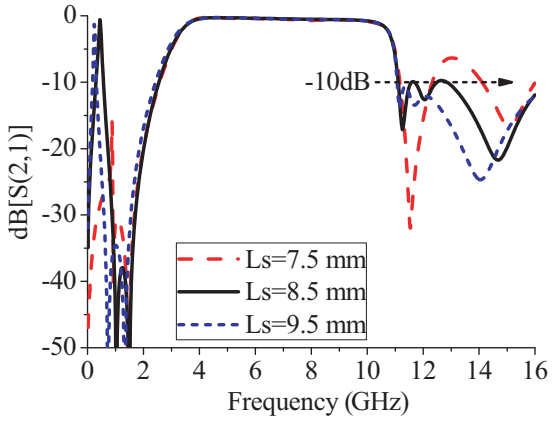

Figure 4. Frequency responses with varied shot-circuit lines length.

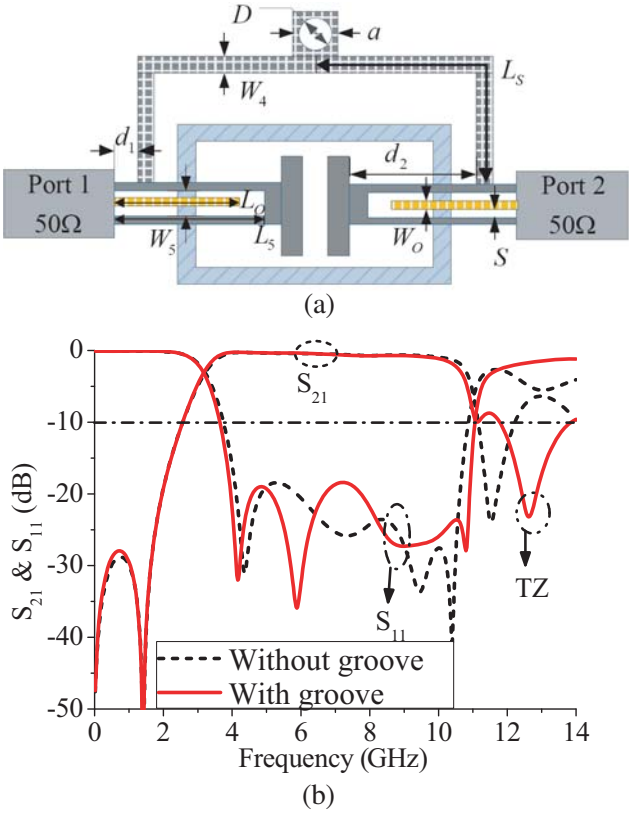

Figure 5. (a) Layout of ultra-wideband-filter with open-circuit-lines to create a stop-band in pass-band. (b) Simulated frequency responses with grooves of size: $W_5 = 1\,\text{mm}$, $L_5 = 6.3\,\text{mm}$ and without grooves.

Based on the above analyses, grooves length L_5 and width W_5 should be appropriately chosen. The simulated frequency responses with adjusted grooves and open-circuit lines size, $L_O = 10.7\,\text{mm}$, $W_O = 0.2\,\text{mm}$, are shown in Fig. 7. As can be remarkably identified, the stopband is centered at 5.8 GHz with its central frequency and relative bandwidth controlled by L_O and W_O. Furthermore, out-of band rejection at right side is greater than 10 dB with left side greater than 27.5 dB and in-band standing waves lower than $-20\,\text{dB}$.

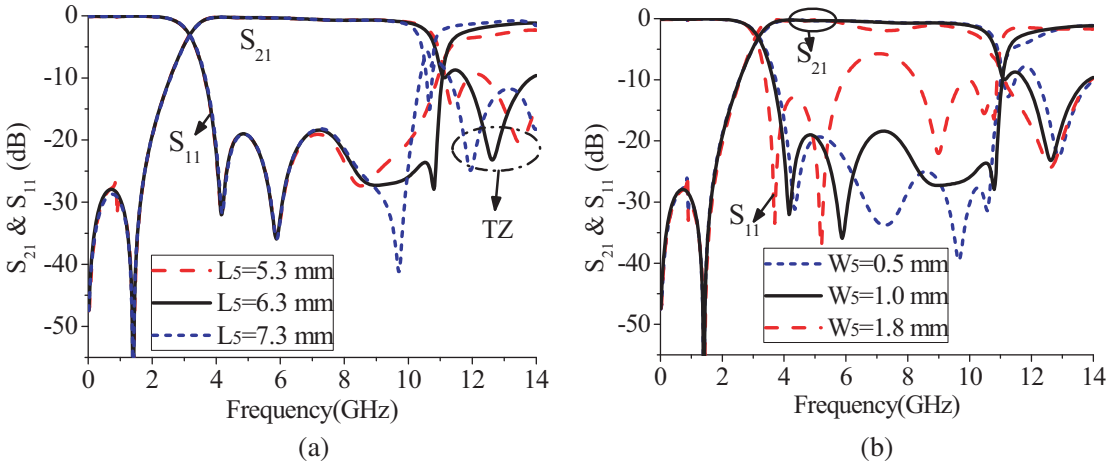

Figure 6. Simulated frequency responses with varied (a) L_5, (b) W_5.

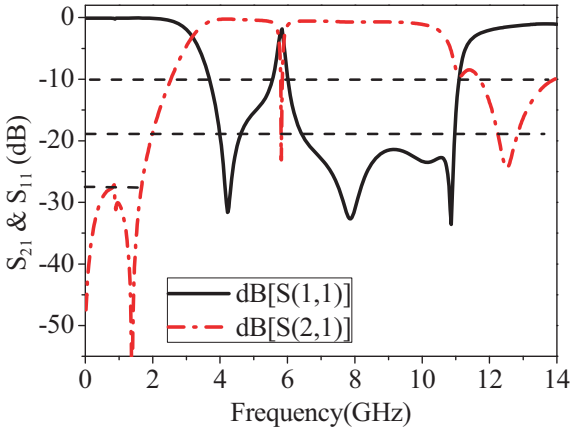

Figure 7. Simulated frequency responses of the UWB BPF with notched band.

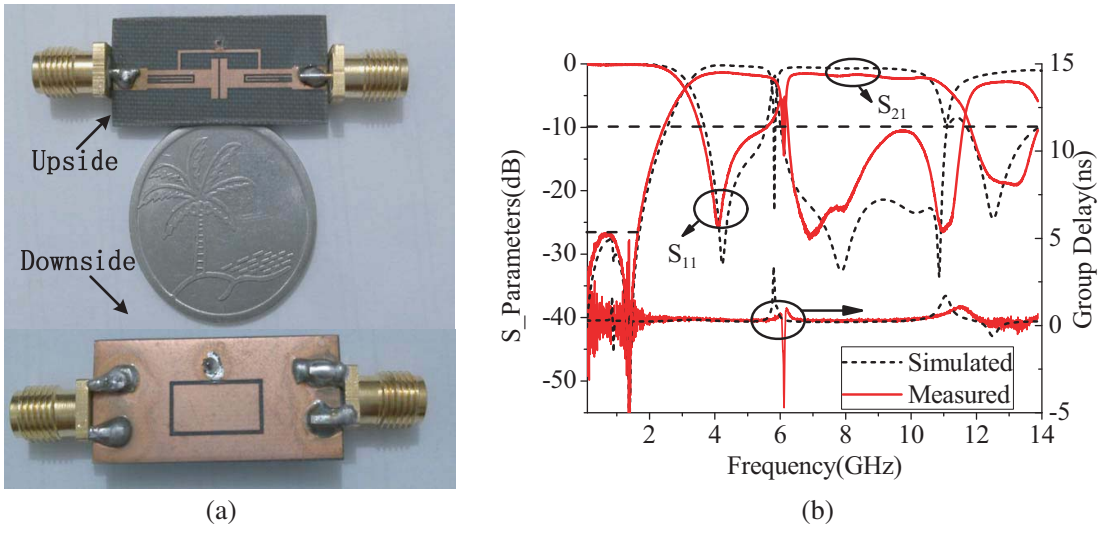

Figure 8. (a) The fabricated UBW BPF. (b) Simulated and measured responses.

3. RESULTS AND DISCUSSION

Experimental results of the UWB filter are directly obtained by means of the Agilent 8719ES vector network analyzer with measuring frequency range from 50 MHz to 13.51 GHz. A photograph of the fabricated filter is given in Fig. 8(a), and simulated and measured results are shown in Fig. 8(b). As can be seen, the experimental results match well with the simulated counterparts. The measured passband is centered at 7.5 GHz with a 3 dB bandwidth of 100%. Within the passband of 3.1–10.6 GHz, the maximum insertion loss is 1.2 dB, while the return loss is higher than 12 dB. Furthermore, the experimental group delay is 0.2 ns, which matches well with the simulated counterparts. The difference between the simulated and measured results is mainly caused by mechanical tolerance issue and the variation of dielectric of the substrate.

4. CONCLUSION

In this letter, a new approach to design ultra-wideband filter using a defected ground structure is composed. After working principle of the proposed filter is explained, an ultra-wideband filter has been designed, fabricated, and measured. The measured results have shown good agreement with simulated ones over a wide frequency range, thus verifying the presented approach and also the theoretically-predicted frequency response.

REFERENCES

1. Gao, X., W. Feng, W. Che, "Compact ultra-wideband bandpass filter with improved upper stopband using open/shorted stubs," *IEEE Microwave and Wireless Components Letters*, Vol. 27, No. 2, 123–125, 2017.
2. Yang, L., Q. Xu, G. Wu, and J. Ye, "Compact ultra-wideband BPF with broad stopband using improved short-circuited coplanar waveguide multiple-mode resonator," *2017 IEEE 2nd Advanced Information Technology, Electronic and Automation Control Conference (IAEAC)*, 2087–2090, 2017.
3. Lu, J. and J. Wang, "Design of compact balanced ultra-wideband bandpass filter with half mode dumbbell DGS," *Electronics Letters*, Vol. 52, No. 9, 731–732, 2016.
4. Gomez-Garcia, R., Raul-Loeches-Sanchez, D. Psychogiou, J.-M. Munoz-Ferreras, and D. Peroulis, "Dual-passband filters and extended-stopband wide-band bandpass filters based on generalized stub-loaded planar circuits," *2017 IEEE MTT-S International Microwave Symposium (IMS)*, 368–371, 2017.
5. Guo, Z. and T. Yang, "Novel compact ultra-wideband bandpass filter based on vialess vertical CPW/microstrip transitions," *Electronics Letters*, Vol. 53, No. 18, 1258–1260, 2017.
6. Kheir, M., T. Kröger, and M. Höft, "A new class of highly-miniaturized reconfigurable UWB filters for multi-band multi-standard transceiver architectures," *IEEE Access*, Vol. 5, 1714–1723, 2017.
7. Zhou, C.-X., P.-P. Guo, K. Zhou, and W. Wu, "Design of a compact UWB filter with high selectivity and superwide stopband," *IEEE Microwave and Wireless Components Letters*, Vol. 27, No. 7, 636–638, 2017.
8. Zhang, T., F. Xiao, and J. Bao, "Compact ultra-wideband bandpass filter with good selectivity," *Electronics Letters*, Vol. 52, No. 3, 210–212, 2016.
9. Janković, N., G. Niarchos, and V. Crnojevi-Bengin, "Compact UWB bandpass filter based on grounded square patch resonator," *Electronics Letters*, Vol. 52, No. 5, 372–374, 2016.
10. Lan, S.-W., M.-H. Weng, C.-Y. Hung, and S.-J. Chang, "Design of a compact ultra-wideband bandpass filter with an extremely broad stopband region," *IEEE Microwave and Wireless Components Letters*, Vol. 26, No. 6, 392–394, 2016.